Clathrate formation by and self-assembled supramolecular structures of a "molecular spring"

Kazuhiko Tanaka,*[a] Hideji Osuga[a] and Yoshinori Kitahara[b]

[a] *Department of Materials Science and Chemistry, Faculty of Systems Engineering, Wakayama University, 930 Sakaedani, Wakayama 640-8510, Japan*
[b] *Department of Chemistry, Graduate School of Science, Kyoto University, Kyoto 606-8224, Japan*

Received (in Cambridge, UK) 26th June 2000, Accepted 15th September 2000
First published as an Advance Article on the web 15th November 2000

The inclusion properties and self-assembly of racemic and optically active helicenediols have been thoroughly investigated. The racemic helicenediol (*PM*-**1**) crystallizes with ethanol or 1,2-dichloroethane in different host–guest stoichiometric ratios to form (*PM*-**1**)·(ethanol) or (*PM*-**1**)$_2$·(1,2-dichloroethane), respectively. Single crystal X-ray analyses of the clathrates show that the helicenediol **1** has greater flexibility to accommodate guest molecules than might have been anticipated. The helical pitch of the helicenediol, which controls the interplanar angle between the terminal thiophene rings, ranges from 38.0, for the ethanol clathrate, to 54.5° for the 1,2-dichloroethane clathrate. This represents an increase of 16.5° or 44%. Testosterone is selectively incorporated into the left-handed helicenediol (*M*-**1**) to afford a 1 : 1 inclusion complex, (*M*-**1**)·(testosterone), in which the interplanar angle decreases from 54.5 to 46.2°. Without guest molecules, racemic helicenediols self-assemble through a unique supramolecular network of hydrogen bonds to form an alternate-leaf motif, while right-handed helicenediols form a four-leaf clover motif in projection. In the self-assembled structures, the interplanar angle of the helicenediol **1** changes from 44.7, for the racemic case, to 33.8° for the right-handed helical case. All of the above evidence points to the surprising conclusion that helicenediol **1** can expand and contract as a "molecular spring". The maximum elongation of the spring is about 61%.

Introduction

There is considerable current interest in the design and construction of highly ordered supramolecular structures, since they could contribute to the development of new materials such as nanoscale molecular devices[1–3] as well as to the synthesis of artificial systems that can mimic biological functions.[4] Among the self-assembled supramolecular architectures such as tapes,[5] sheets,[6] capsules,[7] spheres,[8] squares,[9] cylinders[4] and helices,[9,10] helical arrangements[11,12] are characterized by chirality based on their screw sense, having a right-handed (*P*) or a left-handed (*M*) helicity, and hence the helicoselective (or enantioselective) synthesis of helical motifs is an active field of research in supramolecular chemistry.[1,5,13]

Recently we have described in a brief communication our examinations of the supramolecular helical structures formed by the racemic and optically active helicenediol, 2,13-bis(hydroxymethyl)dithieno[3,2-*e*:3′,2′-*e*′]benzo[1,2-*b*:4,3-*b*′]-bis[1]benzothiophene (**1**)[14] (Fig. 1). We now present in greater detail our results on the nature of the helicenediol **1**, its ability to recognize guest molecules and to self-assemble by adjusting its helical pitch.

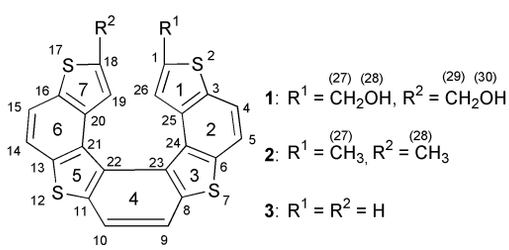

Fig. 1 Numbering scheme of the heterohelicenes (**1**–**3**).

Results

a. Clathrate formation

Recrystallization of the racemic helicenediol (*PM*-**1**) from ethanol yielded an inclusion complex with a 1 : 1 host-to-guest stoichiometric ratio.[15] The clathrate (*PM*-**1**)·(EtOH) is very stable at room temperature, releases the guest molecule at 100 °C and decomposes at 178–183 °C. As shown in Fig. 2, the host molecules of the same helicity are aligned along the crystallographic *b* axis by intermolecular hydrogen bonding to give two homochiral stacking columns, a right-handed strand of (*P*-**1**)·(EtOH) and a left-handed strand of (*M*-**1**)·(EtOH). The columns of the same helicity are interlocked by ethanol molecules through a hydrogen bonding network, with 2.71–2.74 Å the intermolecular O · · · O distance. Each homochiral strand exhibits an alternate-leaf motif with a major diameter of 23.8 Å, where the helicenediol repeats along the *b* axis at a distance of 8.05 Å (Fig. 3).

As can be seen from Fig. 4, benzothiophene ring (ring 4–5) of *PM*-**1** locates on the neighbouring benzodithiophene (ring 5′–4′) with 3.52 Å the shortest C(9)–C(21) distance, indicating the presence of comparatively weak π–π interaction.[16] These π–π stackings and hydrogen bonding fix the alternate-leaf motif, thus rendering the structure completely rigid. The interplanar angle between two terminal thiophene rings of (*PM*-**1**)·(EtOH) is 38.0°.

When the racemic helicenediol was recrystallized from 1,2-dichloroethane, orange clathrate crystals with a 2 : 1 host-to-guest stoichiometry, (*PM*-**1**)$_2$·($ClCH_2CH_2Cl$) (mp 174–177 °C), were obtained. X-Ray crystal analysis of the clathrate shows that a right-handed helicenediol interacts with a left-handed helicenediol by H-bonding to form a heterochiral dimer as

 DOI: 10.1039/b005070i

Table 1 Crystallographic data and structure refinement information

	PM-**1**	*P*-**1**	(*PM*-**1**)·(EtOH)	(*PM*-**1**)$_2$·($ClCH_2CH_2Cl$)	(*M*-**1**)·(testosterone)	*PM*-**2**
Formula	$C_{24}H_{14}O_2S_4$	$C_{24}H_{14}O_2S_4$	$C_{26}H_{20}O_3S_4$	$C_{25}H_{16}ClO_2S_4$	$C_{43}H_{42}O_4S_4$	$C_{24}H_{14}S_4$
Formula weight	462.61	462.61	508.68	512.09	751.04	430.61
a/Å	15.217	11.4866	15.028	8.612	9.724	10.715
b/Å	33.919		8.046	29.042	17.123	11.3870
c/Å	7.85	15.493	19.369	18.387	11.515	8.308
α/°						93.30
β/°			102.779	101.77	103.278	105.42
γ/°						89.685
V/Å^3	4051	2044.1	2284.0	4502	1866.0	975.4
Temperature/°C	20	25	20	26	20	16
Space group	*Pccn*	$P4_3$	$P2_1/c$	$P2_1/n$	$P2_1$	$P\bar{1}$
Z	8	4	4	8	2	2
μ/cm^{-1}	44.72	44.31	40.52	51.49	26.78	45.18
No. of reflections measured	3477	3536	3828	7105	6147	3061
No. of observations	1588 ($I > 2.00\sigma(I)$)	1538 ($I > 3.00\sigma(I)$)	2792 ($I > 3.00\sigma(I)$)	4262 ($I > 3.00\sigma(I)$)	2630 ($I > 2.00\sigma(I)$)	2637 ($I > 3.00\sigma(I)$)
No. of variables	278	271	347	662	464	278
R	0.085	0.032	0.046	0.052	0.043	0.040
*R*w	0.111	0.050	0.055	0.055	0.068	0.074

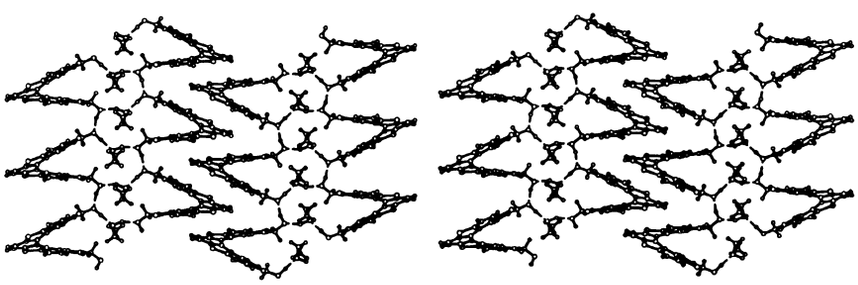

Fig. 2 Stereoview of the hydrogen bonding network of (*PM*-**1**)·(EtOH). Ethanol molecules join two stacking columns of the same helicity to form two stacking columns of (*P*-**1**)·(EtOH) (left side) and (*M*-**1**)·(EtOH) (right side).

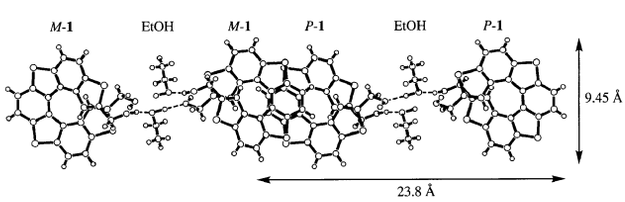

Fig. 3 Top view of two neighbouring stacking columns of (*PM*-**1**)·(EtOH) looking down the *b* axis. The central benzene rings of *P*-**1** and *M*-**1** are alternately piled up along the *b* axis.

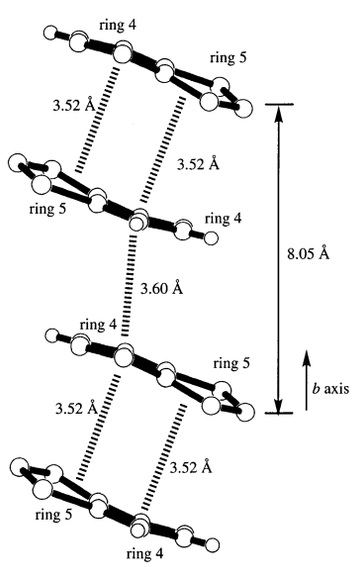

Fig. 4 Molecular overlapping of the central aromatic rings of neighbouring enantiomers in the crystal (*PM*-**1**)·(EtOH).

shown in Fig. 5. One of the hydroxy groups of one enantiomer in the heterochiral dimer locates between two hydroxy groups of the opposite enantiomer by hydrogen bonding. This arrangement extends the interplanar angle from 38.0 to 54.5°. It is noteworthy that 1,2-dichloroethane locates in the canal, aligned along the *a* axis, but there is no interaction between the guest molecules. Since the distances between the two chlorine atoms of 1,2-dichloroethane and the benzene rings of the helicenediol are 3.4 and 3.5 Å (Fig. 6), Cl–π interactions[17] must play an essential role in stabilizing this inclusion complex. The shortest host–guest C···Cl interaction is 3.44 Å and the shortest distance between the Cl atoms and the C atom of the adjacent guest molecule is 4.06 Å. In the canal, the Cl–C–C–Cl dihedral angle is 178.8°, indicating the most stable *anti* conformation.

Racemic 1,18-dimethylhelicene (*PM*-**2**) was prepared by non-photochemical methods utilizing Ullman and McMurry coupling reactions from 1-methylbenzo[1,2-*b*:4,3-*b*′]dithiophene as a starting material.[18] Recrystallization of *PM*-**2** from hexane–benzene gave guest-free crystals suitable for X-ray analysis. The stereoview of the crystal structure of *PM*-**2** is shown in Fig. 7, where right-handed and left-handed dimethylhelicenes arrange alternately along the *a* axis to form a staircase-like motif. Since the dibenzothiophene framework of one enantiomer is situated close to the neighbouring dibenzothiophene framework of *PM*-**2** with a distance of 3.32–3.39 Å, there must be π–π interaction[16] between the two enantiomers. It should be pointed out that the interplanar angle of *PM*-**2** (46.9°) is very close to those of unsubstituted thiaheterohelicenes (45.9 and 48.6°).[19]

When a suspension containing equimolar amounts of enantiomerically pure helicenediol (*M*-**1**) and testosterone was refluxed in acetone–benzene, and the clear solution allowed to cool, an orange crystalline inclusion complex (mp 185–187 °C) with a 1 : 1 stoichiometry was formed. It is important to point out

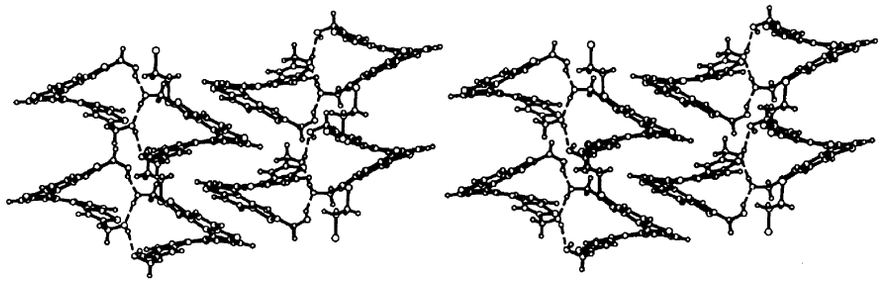

Fig. 5 Stereoview of the heterochiral dimer of *P*- and *M*-helicenediols in the clathrate (*PM*-**1**)$_2$·(1,2-dichloroethane).

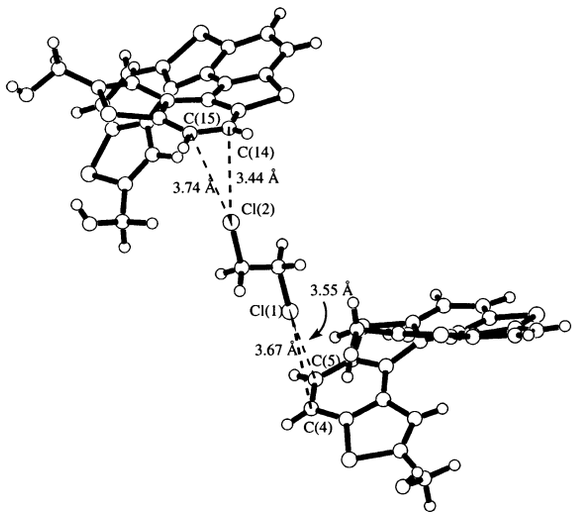

Fig. 6 Crystal structure of the clathrate (*PM*-**1**)$_2$·(1,2-dichloroethane).

that no clathrate was isolated from the racemic or the right-handed helicenediol with other steroids such as methyltestosterone, progesterone, androsterone, and estrone under the same conditions as those of the reaction of *M*-**1** and testosterone. The structure of (*M*-**1**)·(testosterone) is shown in Fig. 8, where the carbonyl and hydroxy functions of testosterone are interlocked by hydrogen bonding to align themselves along the *b* axis (2_1-axis) forming a the head-to-tail hydrogen bonded network. This hydrogen bonding pattern of testosterone in the crystal structure is a common feature in steroids such as *d*-norgestrel,[20a] estriol,[20b] cholanamide,[20c] and cholic acid.[20d] Although the hydroxy groups of the helicenediol are disordered in the crystal lattice, and hence their positions and orientations are known with relatively low precision, it is safe to say that the left-handed helicenediol stacks between the networks of testosterone, and the two methyl groups of testosterone are close to the helicenediol with 3.36 and 3.23 Å (Me)H · · · C distances. The axial hydrogen atoms are close to the benzene and thiophene rings of the helicenediol with distances of 3.0–3.1 Å as shown in Fig. 8. These interactions and hydrogen bonding between *M*-**1** and testosterone may be operative in the inclusion selectivity of *M*-**1**. The interplanar angle (46.2°) of (*M*-**1**)·(testosterone) is very close to that of dimethylhelicene *PM*-**2**.

b. Self-assembled supramolecular structures

Recrystallization of *PM*-**1** from acetone or benzene gave guest-free crystals of *PM*-**1**, where one enantiomer interacts with the opposite enantiomer by H-bonding to form two heterochiral stacking columns (Fig. 9). This H-bonded strand constitutes an alternate-leaf motif with a glide plane, and runs parallel along the *c* axis at a fixed distance, providing a supramolecular column of 7.85 Å pitch and 18.5 × 8.4 Å width (Fig. 10). The distance between the two benzene rings (4 and 4′) in the alternate-leaf motif is 3.24–3.49 Å, which is in the region of stable π–π interaction.[16] The dihedral angle between the two terminal rings of *PM*-**1** is 44.7°.

Crystals of the enantiomerically pure helicenediol (*P*-**1**)[14] were grown from a dichloromethane–acetone solvent mixture. The stereoview of the crystal structure is shown in Fig. 11, where *P*-**1** self-assembles through a right-handed helical network of hydrogen bonding, forming a *four-leaf clover* motif in projection. A full turn of the helicate comprises four chiral leaves and the pitch of the helix is 15.49 Å. The most remarkable feature of *P*-**1** is that the right-handed helicenediols arrange in a *left-handed* helical manner to give a double helical structure and the clover leaf motif in projection repeats by the 4_3 screw axis. In this supramolecular structure, one of the hydroxy functionalities of *P*-**1** interacts with the other hydroxy group of the same molecule and also interacts with one of the hydroxy groups of an adjacent molecule (Fig. 12). Chiral helicenediol exhibits the smallest dihedral angle of the eight crystal structures examined.

Discussion

It is of interest to compare the alignment of an unfunctionalized helicene with that of a bifunctionalized helicene in the crystal lattice. Thus, the racemic dimethylhelicene (*PM*-**2**) shows a marked tendency to form a layered structure consisting of alternating left-handed *and* right-handed enantiomers, providing a $(PM)_n$ column. In contrast, the racemic bis(hydroxymethyl)helicene (*PM*-**1**) prefers specific aggregate structures consisting of either left-handed or right-handed enantiomers, forming homochiral strands such as $(P)_n$- and $(M)_n$-strands. However, the dihedral angles of bifunctionalized helicenes such as the dimethylhelicene **2** and the unsubstituted helicene **3** are 46–49°. Thus, in the case of the bifunctionalized helicene **1**, the host–guest and host–host interactions are crucial to the change of the helical pitch.

Because of a severe interaction between terminal thiophene rings, the distortion from planarity locates on the central aromatic rings of the helical framework (Table 2). Thus, the carbon–carbon bond distances of the outer rings [C(4)–C(5), C(9)–C(10) and C(14)–C(15)] are shortened to 1.34–1.37 Å and the inner carbon–carbon bond distances [C(20)–C(21), C(22)–C(23) and C(24)–C(25)] are lengthened to 1.41–1.43 Å, as shown in Table 3. The inner carbon–carbon bond lengths in the thiophene rings [C(19)–C(20), C(21)–C(22) and C(25)–C(26)] are 1.43–1.47 Å, slightly longer than those of a thiophene molecule (1.43 Å).[21] The common feature of these helical geometries is that the carbon–sulfur bond distances in the thiophene rings are uniformly lengthened from 1.71 to 1.73 Å. Although there are no significant variations in the interatomic C(19)–C(26) distances as shown in Table 4, interatomic C(27)–C(29) distances vary considerably from 4.37, for *P*-**1**, to 5.77 Å for (*PM*-**1**)$_2$·($ClCH_2CH_2Cl$), a remarkable increase of 1.4 Å or 32%. Moreover, as indicated in Table 2, the interplanar angles, which control the pitch of the helix, vary from 33.8, for *P*-**1**, to 54.5° for (*PM*-**1**)$_2$·($ClCH_2CH_2Cl$). Thus a dramatic increase of 20.7° or 61% is observed across the range of compounds studied, indicating that the framework of helicenediol exhibits

Table 2 Dihedral angles between adjacent aromatic rings (°)

	(*PM*-**1**)·(EtOH)	(*PM*-**1**)$_2$·(1,2-dichloroethane)[a]		*PM*-**1**	*PM*-**2**	*P*-**1**	(*M*-**1**)·(testosterone)	*PM*-**3**[b]	*P*-**3**[b]
Ring(1)–Ring(2)	8.29	7.03	8.88	5.82	8.93	8.40	8.90	8.8	6.4
Ring(2)–Ring(3)	8.29	10.76	8.91	7.70	10.19	6.92	8.63	8.6	7.3
Ring(3)–Ring(4)	11.63	13.37	10.13	10.46	11.22	9.73	9.75	11.3	11.6
Ring(4)–Ring(5)	9.23	10.54	13.13	12.72	10.48	9.35	12.82	11.3	12.4
Ring(5)–Ring(6)	7.10	10.12	11.08	9.84	8.22	8.73	9.29	8.6	9.0
Ring(6)–Ring(7)	7.30	8.16	9.17	6.61	8.89	6.33	6.49	8.8	6.7
Ring(1)–Ring(7)	38.0	54.5	52.2	44.7	46.9	33.8	46.2	48.6	45.9

[a] Two independent molecules of helicenediol exist in the crystal lattice; $P2_1/n$, $Z = 8$. [b] For the crystal structure of the racemic and enantiomerically pure heterohelicenes **3**, see ref. 19.

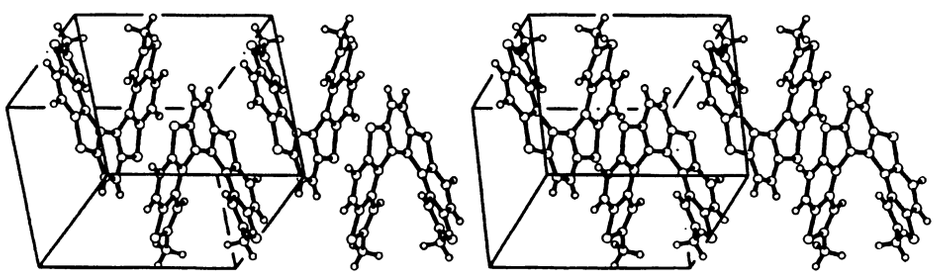

Fig. 7 Stereoview of the crystal packing of the dimethylhelicene *PM*-**2**. The right-handed and left-handed dimethylhelicenes arrange alternately along the crystallographic *a* direction.

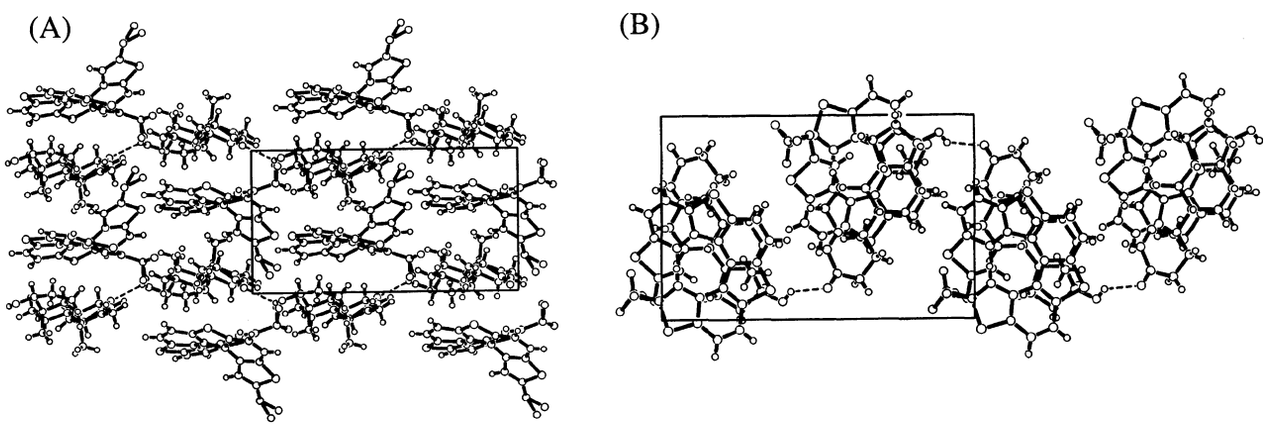

Fig. 8 The 2-D crystalline packing arrangement of (*M*-**1**)·(testosterone) looking down the crystallographic *c* axis (A) and *a* axis (B). The terminal methylene carbons of *M*-**1** have two and three disordered oxygen atoms.

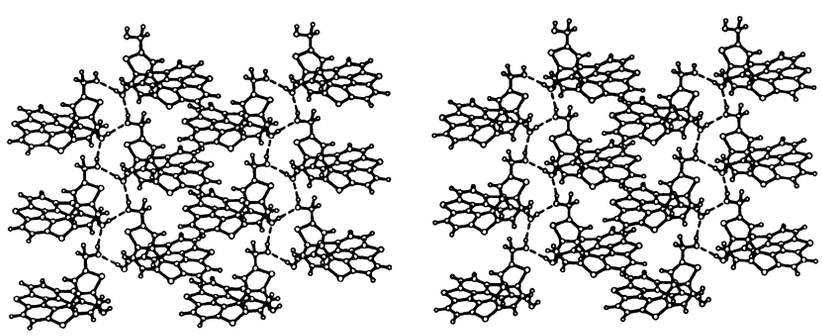

Fig. 9 Stereoview of the crystal *PM*-**1**, showing two neighbouring hydrogen bonded columns.

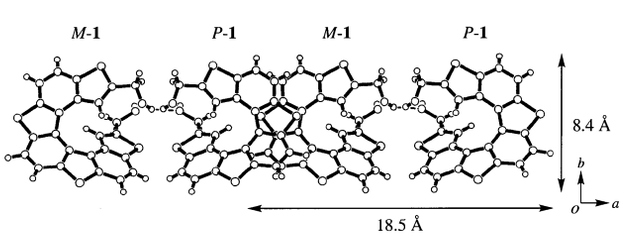

Fig. 10 Top view of neighbouring columns in the crystal of *PM*-**1** showing the overlapping benzodithiophene rings.

significant *elasticity*. This intriguing feature can be visualized by the ORTEP structures in Fig. 13.

Conclusions

We have demonstrated a unique set of crystal structures based on the ability of helicenediol to engage in both clathrate formation and supramolecular self-assembly by hydrogen bonding. The most outstanding conclusion of our work is that the helical conjugated π-electron framework is flexible and that helicene-

Table 3 Average bond distances (Å) of helicenes **1** and **2**

Average distance	(*PM*-**1**)·(EtOH)	(*PM*-**1**)$_2$·(1,2-dichloroethane)	*PM*-**1**	*P*-**1**	(*M*-**1**)·(testosterone)	*PM*-**2**
Outer C–C bond distance[a]	1.36	1.37	1.34	1.34	1.36	1.36
Inner C–C bond distance[b]	1.43	1.42	1.42	1.42	1.41	1.42
Inner C–C distance of thiophene[c]	1.44	1.44	1.44	1.45	1.44	1.45
C–S distances of thiophene[d]	1.73	1.73	1.73	1.74	1.73	1.74

[a] Average of bonds C(4)–C(5), C(9)–C(10) and C(14)–C(15). [b] Average of bonds C(20)–C(21), C(22)–C(23) and C(24)–C(25). [c] Average of bonds C(19)–C(20), C(21)–C(22), C(23)–C(24) and C(25)–C(26). [d] Average of bonds C(1)–S(2), S(2)–C(3), C(6)–S(7), S(7)–C(8), C(11)–S(12), S(12)–C(13), C(16)–S(17) and S(17)–C(18).

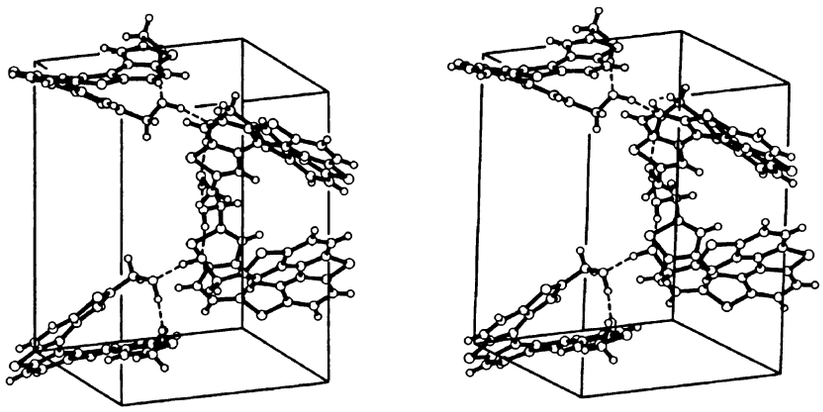

Fig. 11 Stereoview of the unit cell of the crystal *P*-**1**. Inter- and intramolecular hydrogen bonding is shown as dashed lines.

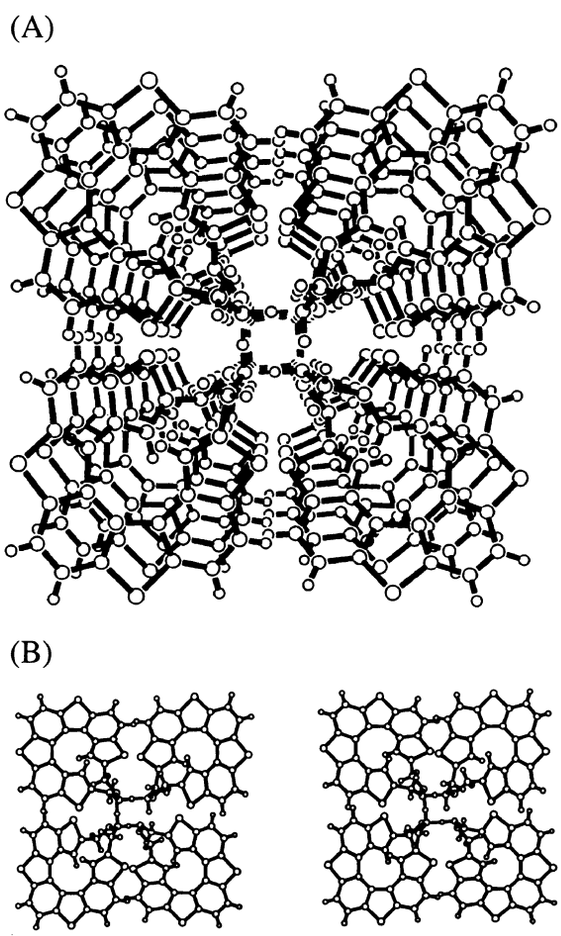

Fig. 12 (A): Top view of the left-handed helical network of *P*-**1**. (B): Stereoview from the screw axis of the four-leaf clover motif in projection.

diol acts as a "molecular spring" according to the patterns of hydrogen bonded networks with itself and with guest molecules. Moreover, the left-handed helicenediol shows a high affinity to testosterone, forming a stable inclusion complex. Since the structures of host–guest complexes in the solid state may differ from the structures in solution, we are continuing to synthesize and study bridged helicenes with fixed helical pitches, in order to better understand molecular recognition in solution. The results of these studies will be reported in due course.

Experimental

Single crystals of (*PM*-**1**)·(EtOH), (*PM*-**1**)$_2$·(1,2-dichloroethane), dimethylhelicene (**2**), *PM*-**1** and *P*-**1** were obtained by recrystallization from the following solvents; ethanol, 1,2-dichloroethane, hexane–1,2-dichloroethane, acetone and dichloroethane, respectively. From an acetone solution of a 1:1 mixture of *M*-**1** and testosterone, the clathrate (*M*-**1**)·(testosterone) was obtained by the slow addition of benzene. Data were collected by a Rigaku AFC7S diffractometer with Cu–Kα radiation, and the structures solved and refined using the TEXSAN crystallographic program package of the Molecular Structure Corporation. The hydrogen atoms of non-hydroxy groups in the crystal (*PM*)-**1**, of 1,2-dichloroethane in the crystal (*PM*-**1**)$_2$·(1,2-dichloroethane) and of the methyl groups of the crystal **2** were placed in calculated positions and added as fixed contributions. The absolute structure and space group of crystal *P*-**1** were established by structure refinement using Bijvoet-pair reflections (Flack *x* parameter = 0.0364 with esd 0.0168). In the crystal (*M*-**1**)·(testosterone), the two oxygen atoms of the helicenediol are disordered. The oxygen atoms connected with C(27) were refined with site occupancy of 0.58 and 0.42, and the others with C(29) were 0.56, 0.25 and 0.19 to have same value of B_{eq}; $8\pi(U_{11}(aa^*)^2 + U_{22}(bb^*)^2 + U_{33}(cc^*)^2 + 2U_{12}aa^*bb^*\cos\gamma + 2U_{13}aa^*cc^*\cos\beta + 2U_{23}bb^*cc^*\cos\alpha)/3$. Thermal parameters for these oxygen atoms were kept isotropic. All other non-hydrogen atoms were refined with anisotropic thermal parameters. Final atomic coordinates, bond lengths, and bond angles for all structures are given in the supplementary information.†

† CCDC reference number 188/273. See http://www.rsc.org/suppdata/p2/b0/b005070i for crystallographic files in .cif format.

Table 4 Selected non-bonded atom–atom distances (Å) of terminal thiophene rings

	(*PM*-**1**)·(EtOH)	(*PM*-**1**)$_2$·(1,2-dichloroethane)[a]		*PM*-**1**	*PM*-**2**	*P*-**1**	(*M*-**1**)·(testosterone)	*PM*-**3**[b]	*P*-**3**[b]
C(19)–C(26)	2.94	3.09	3.11	2.98	3.08	2.84	2.99	3.01	2.96
C(19)–C(25)	3.05	3.13	3.07	3.09	3.10	3.02	3.03	3.12	3.14
C(20)–C(26)	3.11	3.14	3.11	3.10	3.11	3.05	3.12	3.12	3.14
C(1)–C(19)	3.58	3.88	3.91	3.67	3.85	3.47	3.68	3.79	3.71
C(1)–C(18)	3.83	4.32	4.32	4.03	4.17	3.65	4.05	4.17	4.04
C(27)–C(29)	4.73	5.76	5.77	5.14	5.44	4.37	5.16		
O(28)–O(30)	5.70	4.98	4.91	5.20		2.78			

[a] Two independent molecules of helicenediol exist in the crystal lattice; $P2_1/n$, $Z = 8$. [b] For the crystal structure of the racemic and enantiomerically pure heterohelicenes **3**, see ref. 19.

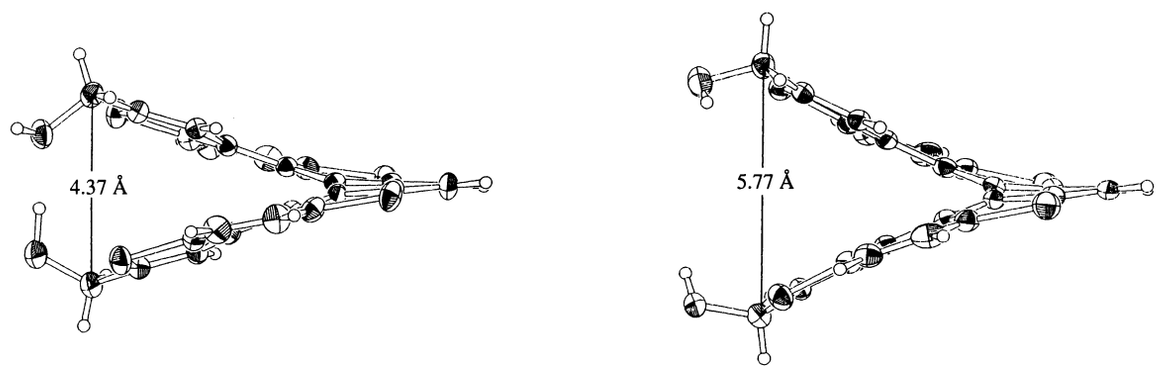

Fig. 13 ORTEP drawing of helicenediol in crystals *P*-**1** (left) and in the clathrate (*PM*-**1**)·(1,2-dichloroethane) (right).

Acknowledgements

This work was supported by Grants-in-Aid for Exploratory Research (No. 11875212), Scientific Research (B) (No. 12440179), and Encouragement of Young Scientists (No. 11740353) from the Ministry of Education, Science, Sports and Culture. Y. K. acknowledges support from the Japan Society for the Promotion of Science (No. 4561). H. O. acknowledges financial support from the Sumitomo Foundation.

References

1 J.-M. Lehn, *Angew. Chem.*, *Int. Ed. Engl.*, 1990, **29**, 1304.
2 G. R. Desiraju, *Angew. Chem.*, *Int. Ed. Engl.*, 1995, **34**, 2311.
3 C. Piguet, J.-C. Bünzli, G. Bernardinelli, G. Hopfgartner, S. Petoud and O. Schaad, *J. Am. Chem. Soc.*, 1996, **118**, 6681.
4 M. R. Ghadiri, J. R. Granja and L. K. Buehler, *Nature*, 1994, **369**, 301.
5 J. C. MacDonald and G. M. Whitesides, *Chem. Rev.*, 1994, **94**, 2383.
6 M. M. Conn and J. Rebek, Jr., *Chem. Ber.*, 1997, **97**, 1647.
7 M. Fujita, D. Oguro, M. Miyazawa, H. Oka, K. Yamaguchi and K. Ogura, *Nature*, 1995, **378**, 469.
8 J. Manna, J. C. Kuel, J. A. Whiteford, P. J. Stang, D. C. Muddiman, S. A. Hofstadler and R. D. Smith, *J. Am. Chem. Soc.*, 1997, **119**, 11611.
9 D. M. Bassani, J.-M. Lehn, G. Baum and D. Fenske, *Angew. Chem.*, *Int. Ed. Engl.*, 1997, **36**, 1845.
10 P. N. W. Baxter, H. Sleiman, J.-M. Lehn and K. Rissanen, *Angew. Chem.*, *Int. Ed. Engl.*, 1997, **36**, 1297.
11 Y. Hamuro, S. J. Geib and A. D. Hamilton, *J. Am. Chem. Soc.*, 1997, **119**, 10587.
12 A. Williams, *Chem. Eur. J.*, 1997, **3**, 15.
13 C. Piguet, G. Bernardinelli and G. Hopfgartner, *Chem. Rev.*, 1997, **97**, 2005.
14 K. Tanaka and Y. Kitahara, *Chem. Commun.*, 1998, 1141.
15 K. Tanaka, Y. Shogase, H. Suzuki, W. Nakanishi, K. Nakamura and Y. Kawai, *J. Chem. Soc.*, *Chem. Commun.*, 1995, 1873.
16 (*a*) C. A. Hunter and J. K. M. Sanders, *J. Am. Chem. Soc.*, 1990, **112**, 5525; (*b*) C. A. Hunter, *Chem. Soc. Rev.*, 1994, 101; (*c*) C. H. Suresh and S. R. Gadre, *J. Org. Chem.*, 1999, **64**, 2505.
17 (*a*) A. Irving, *Supramol. Chem.*, 1997, **8**, 267; (*b*) A. Irving and H. M. N. H. Irving, *J. Crystallogr. Spectrosc. Res.*, 1993, **23**, 725; (*c*) G. R. Desiraju, *Chem. Commun.*, 1997, 1475.
18 K. Tanaka, H. Suzuki and H. Osuga, *Tetrahedron Lett.*, 1997, **38**, 457.
19 H. Nakagawa, A. Obata, K.-i. Yamada and H. Kawazura, *J. Chem. Soc.*, *Perkin Trans. 2*, 1985, 1899.
20 (*a*) N. J. DeAngels, T. H. Doyne and P. L. Grob, *Acta Crystallogr. Sect. B*, 1975, **31**, 2040; (*b*) A. Cooper, D. A. Norton and H. Hauptman, *Acta Crystallogr. Sect. B*, 1969, **25**, 814; (*c*) P. J. Roberts, R. C. Pettersen, G. M. Sheldrick, N. W. Isaacs and O. Kennard, *J. Chem. Soc.*, *Perkin Trans. 2*, 1973, 1978; (*d*) K. Sada, T. Maeda and M. Miyata, *Chem. Lett.*, 1996, 837.
21 B. Bak, D. Christensen, L. Hansen-Nygaard and J. Rastrup-Andersen, *J. Mol. Spectrosc.*, 1961, **7**, 58.